Plastic Stress–Strain History at Notch Roots in Tensile Strips under Monotonic Loading

Predictions of net-section stress and notch strain calculated from the Neuber and Hardrath-Ohman theories are compared with measurements made on notched tensile strips under monotonically increasing loading

by Ralph Papirno

ABSTRACT—Various authors have proposed analytic relations for predicting the plastic behavior at the root of a notch. Among these are relations by Neuber and by Hardrath and Ohman, the latter having generalized on earlier work by Stowell. These methods have had limited experimental confirmation and it was the objective of the investigation reported herein to assess the predictive value of each of the two theories by comparison with test data on externally notched tensile specimens, monotonically loaded to large strains.

Since maximum notch-root strain and net-section stress are the only parameters which can be directly measured in a test, theoretical predictions of these same parameters were developed. This was done using a piece-wise analytical representation of the stress–strain curve. Computer programs were developed for analyzing the stress–strain data and for computing the theoretical results.

A comparison of theory with tests on flat, notched specimens of AISI 4340 steel, heat treated, with initial elastic concentration factors of 1.5 to 2.0 showed a systematic discrepancy which is attributed in part to notch strengthening due to triaxial stress. The discrepancy is of the order of 5 percent for the Neuber theory and larger for the Hardrath-Ohman theory for notch strains less than of 0.015 in./in. and becomes progressively larger for both theories at notch strains in excess of 0.015 in./in. For the mild notches studied here, the Neuber theory has better predictive value.

Nomenclature

A_{net} = net section area, in.^{2}
a = exponent
b = notch specimen half gross-width; $b = w/2$, in.
C = coefficient; strain—(strain x stress) power law
C_p = coefficient; $C = C_p$ in plastic region
C_t = coefficient; $C = C_t$ in transition region
d = notch-specimen net-section width, in.
E = modulus of elasticity, psi
E_{sn} = secant modulus at notch root, psi
E_{so} = secant modulus of net section, psi
K_t = theoretical elastic concentration factor
K_ϵ = strain-concentration factor, elastic or plastic
K_σ = stress-concentration factor, elastic or plastic
K_s = elastic concentration factor for a notched semi-infinite plate
l = notch length, in.
m = exponent; $p = m$ in transition region
n = exponent; $p = n$ in plastic region
P = applied load, lb
p = general exponent, strain–(stress x strain) power law
r = notch-root radius, in.
t = specimen thickness, in.
w = notch-specimen gross width, in.
α = exponent, transition region
β = exponent, plastic region
ϵ = strain, in./in.
ϵ_e = elastic strain, in./in.
ϵ_n = maximum notch strain, in./in.
ϵ_o = nominal net-section strain, in./in.
ϵ_p = plastic strain, in./in. [see eq (8)]
ϵ_{pl} = proportional limit strain, in./in.
ϵ_t = transitional strain, in./in. [see eq (7)]
ϵ_y = 0.1-percent offset yield strain, in./in.
λ = exponent, $\lambda = (2m - 1)/m$
μ = exponent, $\mu = (2n - 1)/n$
σ = stress, psi
σ_e = elastic stress, psi
σ_n = maximum notch stress, psi
σ_o = nominal net-section stress, psi; $\sigma_o = P/A_{net}$
σ_p = plastic stress, psi [see eq (9)]
σ_t = transitional stress, psi [see eq (8)]

Ralph Papirno is Research Mechanical Engineer, Theoretical and Applied Mechanics Research Laboratory, Army Materials and Mechanics Research Center, Watertown, Mass. 02172.

Paper was presented at 1971 SESA Spring Meeting held in Salt Lake City, Utah on May 18-21.

Introduction

Development of Plastic Concentration Factors

Two promising approaches to predicting plastic behavior at the roots of notches under monotonic loading are based upon studies originally by Stowell[1] and generalized by Hardrath and Ohman,[2] and a second approach by Neuber.[3] In both of these approaches, the plastic behavior at the notch root was characterized in terms of plastic concentration factors which were, in turn, related to the elastic concentration factor. There is interest in plastic behavior at notches, not only for monotonic loading, but also for low-cycle fatigue. A number of authors have employed plastic concentration factors directly in fatigue studies and, also, to derive fatigue-reduction factors.[4-7]

Stowell[1] determined the plastic stress-concentration factor at a circular hole in an infinite plate. Hardrath and Ohman[2] generalized these results to a variety of geometric discontinuities by relating the plastic concentration factor to the elastic concentration factor and to certain material properties, in a relation given later in this paper as eq (5). Fair to good correlation with experimental data for this relation was presented in Ref. 4 for cyclic loading and in Ref. 8 for monotonic loading.

Neuber[3] related the plastic stress and strain-concentration factors to the elastic concentration factor in a formula which is shown in eq (1) in the next section of this paper. This particular relation was derived in a study of notches under shear loading but Neuber suggested that the relation might also hold in normal loadings. There have been a number of applications of Neuber's relation in cyclic loading.[6-8] Fair to good correlation of the Neuber theory with experimental data for monotonic loading and cyclic loading have been shown by Morrow et al[8] and Impellizzeri[9] using previously published data for aluminum alloy and can also be shown for data on steel reported by Krempl.[10]

Theory vs. Experiment

In experimental monotonic loading tests of notched specimens, two parameters can generally be measured: (a) the net-section stress, from the load and the net area, and (b) the notch strain from strain gages installed at the root of the notch. In comparing theory with experiment, the theoretical results should be developed in the form $f(\sigma_o, \epsilon_n) = 0$, which, in effect, is a predicted notch-strain history. In this form, the theory can be directly related to parameters which can be measured in a test. The results of both theoretical approaches described above and the correlating experimental data have been stated by previous investigators generally in terms of the elastic and plastic concentration factors and have not been stated in terms of the two parameters which can be measured; hence, no rigorous comparisons between predicted and observed loading histories for these theories have been made. Such an evaluation was the subject of the investigation discussed in this paper. The specific objectives were as follows:

1. To derive the relations between net-section stress and notch strain pertinent to both the Neuber and the Hardrath-Ohman theories of notch plastic behavior using an analytical approximation of the virgin material stress-strain curve.

2. To compare theoretical loading histories of net-section stress vs. notch strain with those determined experimentally from tests of externally notched tensile specimens of AISI 4340 steel, heat treated, with elastic concentration factors of 1.5–2.0.

3. To develop computer programs from which the various plastic notch and net-section stress and strain parameters might be calculated for various materials and for arbitrary values of the elastic concentration factors.

In this paper, a general description of the theoretical formulations of Neuber and Hardrath-Ohman is first given, followed by a discussion of a piece-wise analytic approximation of the stress-strain curve. Notch plastic stress and strain relations are next developed by incorporation of the analytic stress-strain relations into the theoretical plastic-concentration-factor relations and a computer program for performing the calculations is described. The experimental program is given in some detail followed by a presentation of experimental and theoretical results. Finally, the predictive values of both theoretical methods are assessed in section on "Conclusions."

Theoretical Formulations

Neuber Theory

The basis of Neuber's approach to predicting plastic concentration factors is in the relation

$$(K_\sigma K_\epsilon)^{1/2} = K_t \tag{1}$$

where, under plane-stress conditions, the concentration factors are defined as

$$K_\sigma = \sigma_n/\sigma_o \quad \text{and} \quad K_\epsilon = \epsilon_n/\epsilon_o$$

Although the original derivation of the Neuber relation resulted from an analysis of a notched specimen in shear, Neuber had suggested that it might also apply to tension and compressive loadings.

In a test of a notched specimen under tension (or compression) loading, it is possible to measure the strain at the root of a notch and to determine the net-section stress from measurements of the applied load and the net-section area. Therefore, theoretical predictions developed from eq (1) if they are to be compared with theory should be in the form:

$$f(\sigma_o, \epsilon_n) = 0 \tag{2}$$

In this way, theory and experiment can be directly compared. By applying the definitions of stress and strain-concentration factor to eq (1), it becomes transformed to

$$(\sigma_o\epsilon_o) K_t^2 = (\sigma_n\epsilon_n) \tag{3}$$

In order to transform eq (3) into the form of eq (2), an analytic representation of the stress-strain properties is required. This is most easily done by the use of the following modified form of the power law of stress-strain behavior:

$$\epsilon = C(\sigma\epsilon)^p \tag{4}$$

In the next section of this paper, it is shown that a piece-wise application of eq (4) can be used to approximate the stress-strain behavior of AISI 4340 steel, the material of interest in this investigation.

Hardrath and Ohman Theory

The generalization of the Stowell relation due to Hardrath and Ohman is of the form

$$K_\sigma = 1 + (K_t - 1)E_{sn}/E_{so} \tag{5}$$

Applying the definitions of plastic stress-concentration factor and secant modulus, eq (5) is transformed to

$$\sigma_n/\sigma_o = 1 + (K_t - 1)\ (\sigma_n/\epsilon_n)\ (\sigma_o/\epsilon_o) \tag{6}$$

It is necessary to transform eq (6) into the form of eq (2), and this can be done by the use of the power law of stress-strain behavior, eq (4) in a piece-wise manner as will subsequently be shown.

Before proceeding further with the development of the theoretical predictions, a description of the piece-wise approximation of the stress-strain curve in the form of eq (4) is given in the next section.

Analytic Stress-Strain Relations for AISI 4340 Steel

A graph of ϵ vs. $(\sigma\epsilon)$ for heat-treated AISI 4340 steel plotted on logarithmic coordinates reveals two linear regions in addition to the elastic region, as

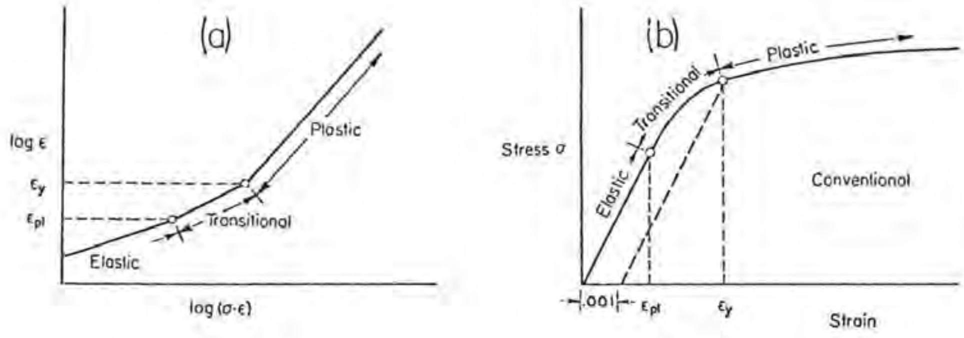

Fig. 1—Log stress, log stress-strain (a) and conventional stress-strain (b) curves for AISI 4340 steel (schematic)

shown schematically in Fig. 1(a). The linear region between the proportional limit strain ϵ_{pl} and the 0.1 percent yield strain ϵ_y has been designated here as the *transitional* region and corresponds to the knee of the conventional stress–strain curve shown in Fig. 1(b). The region where strains are in excess of this yield strain has been designated here as the *plastic* region.

All three regions can be represented by equations of the form given in eq (4):

Elastic	$\epsilon_e = (1/E)^{1/2}\,(\sigma\epsilon)^{1/2}$	(7)
Transitional	$\epsilon_t = C_t(\sigma_t\epsilon_t)^m$	(8)
Plastic	$\epsilon_p = C_p(\sigma_p\epsilon_p)^n$	(9)

A typical log ϵ vs. log $(\sigma\epsilon)$ plot for one heat of heat-treated AISI steel is shown in Fig. 2. An automated data-reduction procedure using a least-squares analysis was applied to obtain the coefficients and exponents shown in the figure. This procedure involved a number of steps: (1) autographic recording of the engineering stress–strain curve; (2) automatic analog-to-digital conversion of the data on punched tape; (3) tape-to-card conversion; (4) computer data reduction using a program which included linear and logarithmic least-squares analyses.

The points ϵ_{pl} and ϵ_y are initially determined from an inspection of the stress–strain curve and these experimental values are employed to set bounds on the three least-squares analyses. When the analyses have been completed and the required constants of eqs (7)-(9) have been determined, the possibility exists that ϵ_{pl} and ϵ_y will not lie on the analytic approximation to the stress–strain curve. The computer program has a provision for solving eq (7) simultaneously with eq (8) for ϵ_{pl} and eq (8) with eq (9) for ϵ_y. The new values of ϵ_{pl} and ϵ_y will lie on the curve and it is these computed values which are employed in the analysis. (The calculated value of ϵ_y may only be an approximation to the 0.1-percent yield strain).

Fig. 2—Log stress, log stress–strain data for one heat of heat-treated AISI 4340 steel showing material constants for three regions

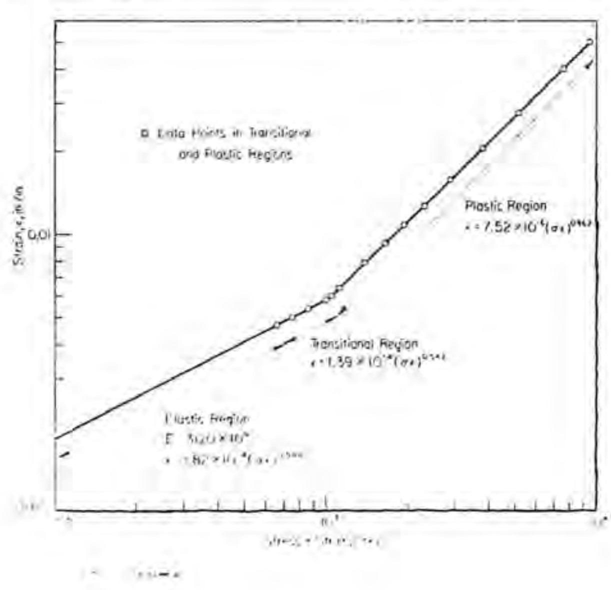

It should be noted that, although a three-part analytic representation of the stress–strain curve was employed in this study in order to achieve a good approximation of the experimentally determined properties of the test material of interest, viz., AISI 4340 steel, in other materials a two-part approximation may be possible. This, in turn, would simplify the necessary calculations somewhat. However, since the calculations can easily be made on a digital computer, such simplification does not appear necessary if a poorer approximation of the stress–strain curve results.

Notch Stress and Strain Analysis

Monotonic-loading Progression

It should be emphasized at the outset that σ_o and ϵ_o are nominal values referring to the net section and are defined as follows:

$$\sigma_o = P/A_{\text{net}} \text{ and } \epsilon_o = f(\sigma_o)$$

In the analysis, it is assumed that σ_o and ϵ_o can be elastic, transitional, or plastic, they are not restricted to the elastic region of the stress–strain curve. On this basis it is possible to recognize six different cases of behavior, net section vs. notch root:

Case No.	Net-Section Condition (Stress)	Notch-Root Condition (Strain)
1	Elastic	Elastic
2	Elastic	Transitional
3	Elastic	Plastic
4	Transitional	Transitional
5	Transitional	Plastic
6	Plastic	Plastic

(If a two-part analytic stress–strain approximation were employed, only cases 1, 3, and 6 would result.)

A given specimen with a predetermined value of the elastic concentration factor will progress through a number of cases as it is loaded monotonically to failure. The actual progression will depend upon the magnitude of K_t and the toughness of the test material. A particular specimen need not progress through all six cases as it is loaded to fracture. For example, with high K_t in a low-toughness material, the progression might be through cases 1, 2, and 3 only; with higher toughness, the progression might be through 1, 2, 3, 5, and 6. Other combinations of toughness and K_t might lead to different progressions.

Net-section Stress vs. Notch-root Strain

By suitable substitutions of eqs (7)-(9) in eq (3), an explicit relation between net-section stress and strain at the notch root can be obtained for the Neuber theory for each of the six cases in the form $\sigma_o = f(\epsilon_n)$. These have been listed below together with the strain boundaries which delineate the specific region of the stress-strain curve for which the particular relation is pertinent.

The Hardrath-Ohman theory can most easily be evaluated by transformation of the implicit stress-strain relations given in eqs (8)-(9) to explicit exponential forms for the two regions:

$$\epsilon = (C_t\sigma^m)^\alpha \quad \text{where} \quad \alpha = 1/(1-m) \qquad (11)$$

$$\epsilon = (C_p\sigma^n)^\beta \quad \text{where} \quad \beta = 1/(1-n) \qquad (12)$$

It is also convenient for calculations using the Hardrath-Ohman theory to use the following substitutions:

$$\lambda = (2m-1)/m \qquad (13)$$

$$\mu = (2n-1)/n \qquad (14)$$

The expressions for cases 1-3 in the Hardrath-Ohman theory can be transformed to the explicit form $\sigma_o = f(\epsilon_n)$ and can be evaluated readily. More complex implicit expression in σ_o and ϵ_n result in cases 4-6 which require a graphical or numerical solution of for σ_o with given values of ϵ_n and vice versa. There are many techniques available for such solutions and these can be readily implemented on a digital computer. A listing of the net-section stress vs. notch-strain relations for cases 1-6 for the Hardrath-Ohman theory follows the listing for the Neuber theory below.

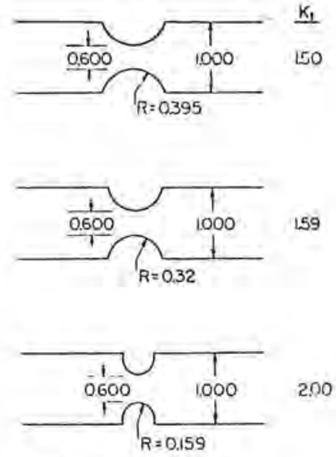

Fig. 3—Notch configurations and dimensions of 0.1-in.-thick flat, notched specimens

pressions, the plastic stress- and strain-concentration factors can be obtained as functions of K_t and the notch stress or strain. As an example, a rather detailed description and listing of such expressions based upon the Neuber theory has previously been given.[11]

Calculation of Theoretical Results

All calculations based upon eqs (15)-(26) were performed on a digital computer. A listing of the program for eqs (15)-(20) is given in Ref. 11. This program has been adapted for eqs (21)-(26) by the addition of a sub-routine for solving the implicit equations given as eq (24)-(26) in the previous listing. In the program, the value of ϵ_n is incremented and calculations are sequentially performed using eqs (15)-(20) or eqs (21)-(16); the choice of the proper equation to be used is determined by testing the strain values according to the prescribed strain limits. In this way, the computations are made only

Neuber Theory

Case No.	Analytic Relation	Strain Boundaries	Eq No.
1.	$\sigma_o = (E/K_t)\epsilon_n$	$0 < \epsilon_n < \epsilon_{pl}$	(15)
2.	$\sigma_o = (E^{1/2}/K_t)\ (\epsilon_n/C_t)^{1/2m}$	$\epsilon_o \leq \epsilon_{pl} < \epsilon_n \leq \epsilon_y$	(16)
3.	$\sigma_o = (E^{1/2}/K_t)\ (\epsilon_n/C_p)^{1/2n}$	$\epsilon_o \leq \epsilon_{pl};\ \epsilon_n > \epsilon_y$	(17)
4.	$\sigma_o = (1/K_t^{(2-2m)})\ (\epsilon_n^{(1-m)}/C_t)^{1/m}$	$\epsilon_{pl} < \epsilon_n < \epsilon_o \leq \epsilon_y$	(18)
5.	$\sigma_o = (1/C_tK_t^{(2-2m)})\ (\epsilon_n/C_p)^{(1-m)/n}$	$\epsilon_{pl} < \epsilon_o < \epsilon_y < \epsilon_n$	(19)
6.	$\sigma_o = (1/K_t^{(2-2n)})\ (\epsilon_n^{(1-n)}/C_p)^{1/n}$	$\epsilon_y < \epsilon_o < \epsilon_n$	(20)

Hardrath-Ohman Theory

Case No.	Analytic Relation	Strain Boundaries	Eq No.
1.	$\sigma_o = (E/K_t)\epsilon_n$	as in eq (15)	(21)
2.	$\sigma_o = E\epsilon_n/(EC_t^{1/m}\epsilon_n^\lambda + K_t - 1)$	as in eq (16)	(22)
3.	$\sigma_o = E\epsilon_n/(EC_p^{1/n}\epsilon_n^\mu + K_t - 1)$	as in eq (17)	(23)
4.	$\sigma_o + (K_t - 1)\ (C_t^\alpha/\epsilon_n)^\lambda\sigma_o^{\alpha m} - (\epsilon_n^{1/\alpha}/C_t)^{1/m} = 0$	as in eq (18)	(24)
5.	$\sigma_o + (K_t - 1)\ (C_t^\alpha/C_p^{1/n}\epsilon^\mu)\sigma_o^{m\alpha} - (\epsilon_n^{1/\beta}/C_p)^{1/n} = 0$	as in eq (19)	(25)
6.	$\sigma_o + (K_t - 1)\ (C_p^\beta/\epsilon_n)^\mu\sigma_o^{\beta n} - (\epsilon_n^{1/\beta}/C_p)^{1/n} = 0$	as in eq (20)	(26)

Typical theoretical results for both theories are given later in this report where they are compared with the results of experiments.

Plastic Concentration Factors and Other Notch Parameters

By suitable substitution of the analytic stress-strain relations into the plastic-concentration-factor ex-

for the pertinent cases for the particular specimen and particular material properties. The resulting output then represents a loading history of the notched specimen. Included in the program is a provision for calculation of the applied load for a specimen of given area with the latter parameter being a part of the input data to the program. A typical output of this program for the Neuber theory has also been given in Ref. 11.

Experimental Procedure

Externally notched flat tension specimens with the notch configurations shown in Fig. 3 were fabricated from two lots of AISI 4340 steel plate. These were given identical heat treatments before specimen fabrication. Electrical-resistance strain gages were installed at the roots of the notches and the specimens were monotonically loaded to fracture. The nominal net-section stress (converted from applied load) and the notch maximum strain were autographically recorded up to approximately 2-percent strain. Stress–strain properties were obtained from standard flat tension specimens. The stress–strain data were recorded autographically and the autographic records were analyzed using the previously outlined automated data-reduction process. The details of the procedure are described in this section; a comparison of the experimental results with the theoretical predictions is given in the next section.

Material

Material-properties specimens and notched specimens were fabricated from two separate heats of AISI 4340 steel plate, received in the annealed condition. Lot No. 1, used for one notched specimen and one smooth tension specimen, was received as 0.5-in.-thick plate, while Lot No. 2 was received as 0.75-in.-thick plate. A standard heat treatment was used which included tempering at 920° F for 1 hr.

The as-received material was cut into blanks from which one or more specimens could later be prepared and heat treated in its full thickness. The thickness was then reduced to 0.10 in. for specimen preparation.

Notch-specimen Preparation and Testing

For the design of the notched specimen shown in Fig. 3 with K_t values of 1.5, 1.59 and 2.00, the following relations, empirically derived by Heywood[12], were employed:

$$K_t = [(l/r)/(1.55[w/d] - 1.3)]^u + 1 \qquad (27)$$

where

$$u = \frac{w/d - 1 + 0.5(l/r)^{1/2}}{w/d - 1 + (l/r)^{1/2}} \qquad (28)$$

(See Fig. 4 for identification of notch parameters.)

After manufacture, the specimens were carefully measured and the actual stress-concentration factors for the notches were re-evaluated using the appropriate formulas. Because of manufacturing tolerances, the values of K_t computed from actual dimensions could depart from the nominal values by several percent.

The basic notch-specimen design is shown in Fig. 5 for one notch configuration. The basic design was used for all the notches shown in Fig. 3. Specimen blanks were cut from the as-received material, heat treated, and then reduced in thickness to 0.10-in. by machining equal amounts of material from each surface. The various holes and contours were machined into the final thickness blank.

Strain gages, BLH Type FAP-03-12, 0.040-in. long and 0.05-in. wide, were cemented at the notch roots, one in each notch in individual specimens. These were electrically connected in series, so that bending components of strain were eliminated and so that the longitudinal strain reading obtained was the average for the two notches in each specimen. The specimen gages formed one arm of a Wheatstone bridge, with compensating gages on a dummy specimen forming an opposite arm. The remainder of the bridge consisted of precision resistors. The unbalance bridge voltage was recorded on a Hewlett-Packard X-Y recorder calibrated to read 0.001-in./in. strain per one-half inch of pen displacement along the recorder X-axis.

The bridge-energizing voltage was held to approximately 2v. This limited the power dissipation of the gages to less than 5 w/sq. in., a sufficiently small value so that excessive heating of the specimen in the notch root was avoided.

Loads were recorded on the Y-axis of the recorder. By taking the specimen area into account, it was possible to calibrate the recorder to read net-section stress directly on a scale where 10 ksi was the equivalent of one-half inch of pen displacement. The resulting autographic recording showed net-section stress as a function of notch strain.

Experimental Accuracy

Load errors (and hence net-section stress errors) were negligible since the testing machine had been calibrated just prior to the testing program using proving rings whose own calibration was traceable to the National Bureau of Standards.

Major sources of error in the strain measurements resulted from an uncertainty of ±3 percent in the value of the gage factor as indicated by the manufacturer. Additional errors are the result of the combined effects of the notch-root tangential strain gradient and possible misalignment of the gage center line with the notch center line. Calculations have

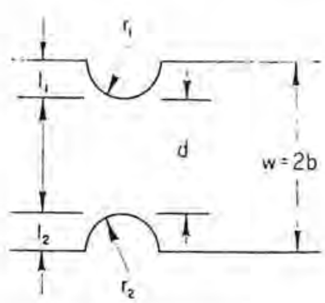

Fig. 4—Identification of notch parameters

Fig. 5—Notch-specimen design and dimensions. Notch configuration dimensions given in Fig. 3

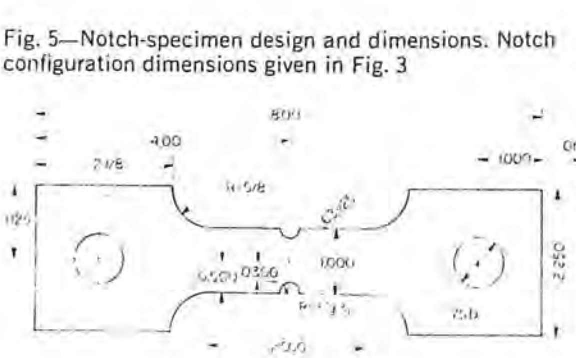

TABLE 1—STRESS–STRAIN DATA FOR TWO HEATS OF HEAT-TREATED AISI 4340 STEEL OBTAINED FROM A LEAST-SQUARES, CURVE-FITTING ANALYSIS

Heat No.	Elastic Modulus, 10^6 psi	ϵ_{pl}, %	ϵ_y, %	Transition Region C_t	m	Plastic Region C_p	n
1	30.0	0.47	0.60	1.39×10^{-4}	0.542	7.25×10^{-6}	0.962
2	29.6	0.53	0.65	0.65×10^{-4}	0.655	7.50×10^{-6}	0.962

shown that both of these effects can result in lower strain-gage readings; however, the error is less than 1 percent.

It was not possible to heat treat all the specimens simultaneously; hence, there may have been small variations in properties between the smooth specimens and the notch specimens and among the smooth specimens themselves. However, the variation of the computed values of notch strain, when the scatter of properties was taken into account, was no more than ±1 percent.

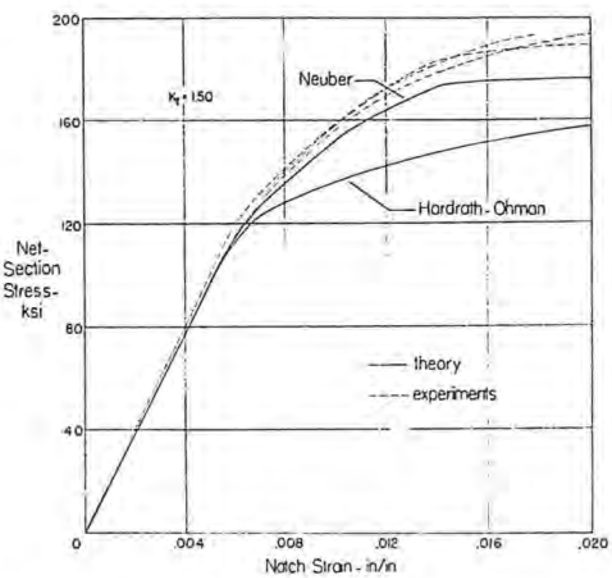

Fig. 6—Net-section stress vs. notch strain for $K_t = 1.5$, experiments and theories

Experimental and Theoretical Results

Mechanical-property Data

The reduced material-property data for the two separate heats of material used for specimen manufacture are given in Table 1. The constants given for transition and plastic regions of the stress–strain curve are those applicable to eqs (7) and (8).

Notch-specimen Data: Experimental and Theoretical

Experimental net-section stress vs. notch-strain data are given in Figs. 6-8 for K_t = 1.5, 1.59 and 2.00, together with theoretical curves derived from eqs (15)-(20) for the Neuber theory and eqs (21)-(26) for the Hardrath-Ohman theory. The experimental data were taken directly from autographic recordings made during the tests, while the theoretical data were developed using the computer program.

Discussion

The discrepancies between the experiments and both theories which are evident especially in Figs. 6 and 8 are larger than those which could result from experimental error. It is significant that, for given

Fig. 7—Net-section stress vs. notch strain for $K_t = 1.59$, experiments and theories

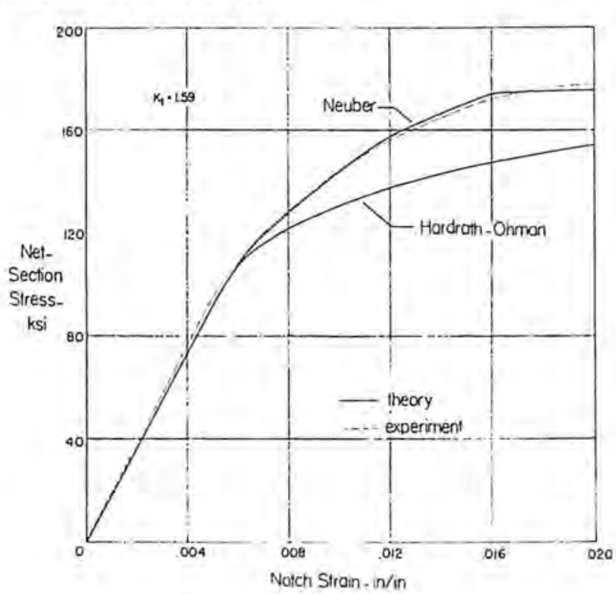

Fig. 8—Net-section stress vs. notch strain for $K_t = 2.0$, experiments and theories

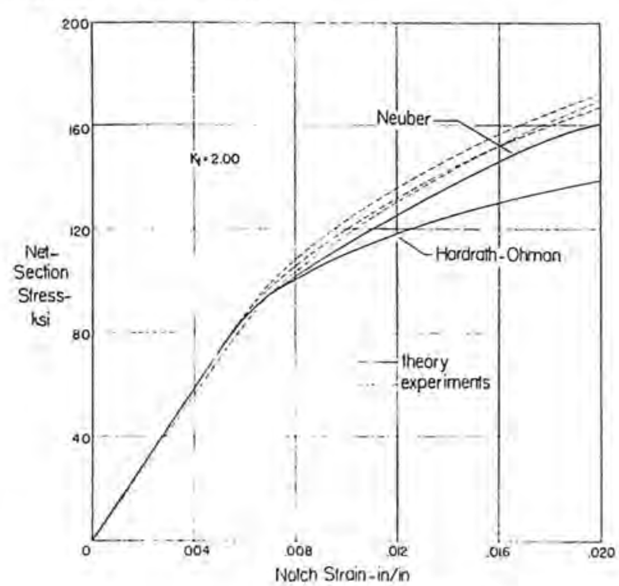

values of notch strain, the experimental net-section stresses are systematically higher than the predictions of either theory and, for strains in excess of approximately 1.5 percent, the discrepancies increase rather markedly. These discrepancies may be due, in part, to notch strengthening in the specimens resulting from the development of triaxial stresses at the notch root. There is additional evidence of notch strengthening in the results of tests to failure of similar notched specimens of the same material. (These tests had been performed prior to the initiation of the study described here.) As shown in Fig. 9, notch-fracture strengths of specimens with initial K_t values of 1.5 to 4.0 are approximately 10 percent higher than the ultimate tensile strength of the virgin material.

In a previously reported comparison of the two theories with test data,[8] the experimental results were converted into strain- and, stress-concentration factors on the assumption that the material at the notch root obeys the virgin-material stress–strain curve, i.e., on the assumption that triaxial stress does *not* develop. As a result, the discrepancies between theory and experiment could not be rationalized.

It would appear that plane-stress conditions in the specimen must be assured into the plastic region, if a more rigorous test of the theories is to be made. There is some question whether this can be done for large plastic strains. Alternatively, it may be possible to modify the theories to take into account the notch strengthening which results from the development of triaxial stress. Both of these alternatives should be pursued.

Within the limitations of both theories in regard to notch strengthening, Figs. 6-8 show that the Neuber theory has better predictive value for the range of K_t studied in this investigation in AISI steel. Net-section stress vs. notch-root-strain calculations were made for $K_t = 2.5$, 3, 4 and 5. It is interesting to note that, for $K_t \sim 2.5$, notch-behavior predictions of both theories virtually coincide, and that, for $K_t > 2.5$, the net-section-stress predictions of the Hardrath-Ohman theory are in excess of those predicted by the Neuber theory. For sharper notches, then, the Hardrath-Ohman theory may have the better predictive value. This suggests a need for further study of notches with values of K_t larger than 2.5.

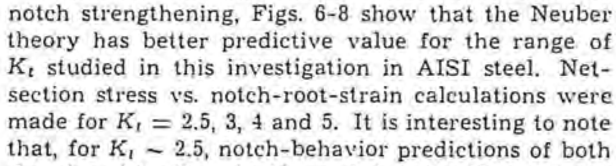

Fig. 9—Strength of flat notched specimens for a range of initial elastic concentration factors

Conclusions

The major conclusions of this study are as follows:

1. Predictions of net-section stress vs. notch strain can be developed for externally notched tensile specimens of AISI 4340 steel using the Neuber and Hardrath-Ohman theories, together with a piecewise analytic representation of the stress–strain curve in three regions: elastic, transitional and plastic.

2. A systematic discrepancy between theoretical and experimental data is observed in which the experimental net-section stress values are in excess of those predicted by either theory. A part of this discrepancy may be due to notch strengthening which results from the development of triaxial stress at the notch root.

3. For the range of K_t of 1.5 to 2.0 in externally notched plate tensile specimens of AISI 4340 steel, the Neuber theory has better predictive value than the Hardrath-Ohman theory.

4. The predicted monotonic loading histories of net-section stress and notch-root strain of both theories coincide for $K_t \sim 2.5$ For $K_t > 2.5$, the predicted net-section-stress values for given transitional and plastic notch-root strains of the Hardrath-Ohman theory are always greater than those of the Neuber theory. This suggests that the Hardrath-Ohman theory may have better predictive value for $K_t > 2.5$ than the Neuber theory.

Acknowledgments

A number of staff members of the Theoretical and Applied Mechanics Research Laboratory contributed to the investigation described herein. John Campo performed the majority of the laboratory tests; John Hannon delicately applied the strain gages in the notch roots and contributed to the development o the automated data-analysis program; Joseph Wong, a summer student aide, and Miss Janet Gorcenski, a Northeastern University co-operative student, assisted with the computer programming and with the calculations. I am grateful to all who contributed and am happy to acknowledge their contributions.

References

1. Stowell, E. Z., "Stress and Strain Concentration at a Circular Hole in an Infinite Plate," NACA TN 2073 (Feb. 1950).
2. Hardrath, H. F. and Ohman, L., "A Study of Elastic and Plastic Stress Concentration Factors Due to Notches and Fillets in Flat Plates," NACA Report 1117 (1953).
3. Neuber, H.,"Theory of Stress Concentration for Shear Strained Prismatical Bodies with Arbitrary Non-linear Stress-Strain Law," Trans. ASME, Jnl. Appl. Mech., 544-550 (Dec. 1961).
4. Crews, J. H. and Hardrath, H. F., "A Study of Cyclic Plastic Stresses at a Notch Root," EXPERIMENTAL MECHANICS, 6 (6), 313-320 (June 1966).
5. Kuhn, P. and Figge, I. E., "Unified Notch Strength Analysis for Wrought Aluminum Alloys," NASA TN D-1259 (May, 1962).
6. Wetzel, R. M., "Smooth Specimen Simulation of Fatigue Behavior at Notches," Jnl. Matls., 3 (3), 646-657 (Sept. 1968).
7. Topper, T. H., Wetzel, R. M. and Morrow, J., "Neuber's Rule Applied to Fatigue of Notched Specimens," Jnl. Matls., 4 (1), 200-209 (March 1969).
8. Morrow, J., Wetzel, R. and Topper, T. H., "Laboratory Simulation of Structural Fatigue Behavior," in Effects of Environment and Complex Load History on Fatigue Life, ASTM STP 462, 74-91 (1970).
9. Impellizzeri, L. F., "Cumulative Damage Analysis in Structural Fatigue," in Effects of Environment and Complex Load History on Fatigue Life, ASTM STP 462, 60-68 (1970).
10. Krempl, E., "Low Cycle Fatigue Reduction in Flat Notched Plates," ASME Preprint 67-Met-13.
11. Papirno, R., "Plastic Concentration Factors in Flat Notched Specimens of AISI 4340 Steel, AMMRC TR 70-72, Army Mats. and Mech. Res. Center (Feb. 1970).
12. Heywood, R. B., Designing by Photoelasticity, Chapman and Hall, Ltd., London, 162-166 (1953).